SLAC–95–6913
June 1995

First Observation of Stimulated Coherent Transition Radiation*

Hung-chi Lihn, Pamela Kung, Chitrlada Settakorn, and Helmut Wiedemann
Applied Physics Department and Stanford Linear Accelerator Center, Stanford University, Stanford, California 94309

David Bocek, and Michael Hernandez
Physics Department and Stanford Linear Accelerator Center, Stanford University, Stanford, California 94309

Stimulated coherent transition radiation has been observed at the Stanford SUNSHINE facility. Far-infrared light pulses of coherent transition radiation emitted from femtosecond electron bunches are delayed and circulated in a special cavity to coincide with subsequent incoming electron bunches. This coincidence of light pulses with electron bunches enables the light work on the electrons, and thus stimulates more radiated energy. The stimulation of radiation is observed via detuning measurements of the cavity and agrees with theoretical predictions. The experimental setup and results will be discussed.

Stimulated transition radiation is emitted when electrons pass through the interface between two media of different dielectric constants with the presence of an external electromagnetic field in phase with the spontaneous transition radiation. The special phase relation enables the external field work on the electrons so that additional energy is extracted from the electrons to the radiation field. This phenomena was predicted in theory several years ago [1,2]. In this Letter, we describe the observation of stimulated transition radiation via detuning measurements of a special cavity. We are able to observe the coherent part of this stimulated radiation, in which wavelengths are longer than or equal to the bunch length [5], in the far-infrared regime via a room-temperature bolometer by utilizing femtosecond electron bunches produced at the Stanford SUNSHINE facility [3,4].

Since Maxwell's equations are linear, the solution to stimulated transition radiation can be split into two linearly independent parts [2]: one part for the external field but without electrons and another for electrons only. The former part is equivalent to Fresnel's equations for reflection and refraction, while the latter part is just spontaneous transition radiation. Let us assume the field solution to the first part is $\mathbf{E}_{ext}$, and the solution to the second part is $\mathbf{E}_{sp}$. Then the field of stimulated transition radiation is $\mathbf{E}_{ext} + \mathbf{E}_{sp}$. Hence, the total radiated power is proportional to $|\mathbf{E}_{ext} + \mathbf{E}_{sp}|^2$. The extra output energy $\Delta\mathcal{E} = |\mathbf{E}_{ext} + \mathbf{E}_{sp}|^2 - |\mathbf{E}_{ext}|^2 - |\mathbf{E}_{sp}|^2 = 2\mathrm{Re}(\mathbf{E}_{ext} \cdot \mathbf{E}^*_{sp})$ is the stimulated radiation that is due to the work done by the external field on electrons [2].

To observe stimulated transition radiation, we use a special cavity named BRAICER (Broadband Radiation Amplifier via Inducing and Circulating Emission of Radiation). The conceptual schematic diagram of the BRAICER cavity is shown in Fig. 1. It consists of a metallic foil radiator/reflector (R), two off-axis parabolic reflectors (P1 and P2), and two plane reflectors (M1 and M2). The focal points of P1 and P2 are aligned with points A and B, respectively. When divergent transition radiation is emitted from A, it becomes parallel after P1. This parallel light is then transported through M1 and M2 to P2, which focuses this parallel light into a point at B. Let us assume the loop length (e.g., A $\rightarrow$ P1 $\rightarrow$ M1 $\rightarrow$ M2 $\rightarrow$ P2 $\rightarrow$ B) is equal to the distance between two adjacent electron bunches of a train of N identical equidistant electron bunches. No loss in the cavity is assumed. When the first bunch passes through A and B, it radiates forward (to the left-hand side) and backward (to the right-hand side) transition radiation. We first focus on the forward radiation (emitted at A). By assuming the emitted field is $\mathbf{E}$, the radiated energy is proportional to $|\mathbf{E}|^2$ in the forward radiation. This radiation travels from A counterclockwise (CCW) to B. As it reaches B, the next incoming electron bunch also arrives at B. Hence, the total radiated field is $\mathbf{E}$ (traveling radiation from the first bunch reflected by R) + $\mathbf{E}$ (spontaneous backward radiation emitted from the second bunch). The radiated energy is now proportional to $|\mathbf{E} + \mathbf{E}|^2 = 4|\mathbf{E}|^2$, and the extra stimulated energy is proportional to $2|\mathbf{E}|^2$. The combined radiation then travels from B clockwise (CW) to A. As it reaches A, the third electron bunch also crosses A. This time, the total radiated field is $2\mathbf{E}$ (traveling radiation from the first and second bunch reflected by R) + $\mathbf{E}$ (spontaneous forward radiation emitted from the third bunch). The radiated energy is then proportional to $|2\mathbf{E}+\mathbf{E}|^2 = 9|\mathbf{E}|^2$, and the extra stimulated energy is proportional to $4|\mathbf{E}|^2$. This process goes on until all N bunches pass through the cavity. The

*Work supported by Department of Energy contract DEAC0376SF00515.

radiated energy after N bunches is proportional to $N^2|\mathbf{E}|^2$. This resonant cavity radiates N times more energy when compared to the total energy radiated from the same N electron bunches through a non-resonant radiator, which is only proportional to $N|\mathbf{E}|^2$. The same process also applies to the backward radiation from the first bunch. Therefore, two independent radiation pulses are traveling in opposite directions through the cavity.

In addition to the resonance mentioned above, the BRAICER cavity also resonates at other loop lengths. When the loop lengths are integral (say n) multiples of the inter-bunch distance d_{ib}, the radiation emitted by an electron bunch travels around the cavity once and meets the next n^{th} incoming bunch. All these resonances described so far are called *first*-order resonances. Similarly, if the loop lengths are half-integral (say $n/2, n$ odd) multiples of d_{ib}, the radiation emitted by a bunch must travel around the cavity twice (e.g., $\mathsf{A} \xrightarrow{CCW} \mathsf{B} \xrightarrow{CW} \mathsf{A}$) to meet the next n^{th} incoming bunch. These are categorized as *second*-order resonances. Thus, the order of resonance is defined by the number of loops traveled around the cavity necessary for the light pulse to meet a subsequent electron bunch. If there are no cavity losses, these different orders of resonances reach amplitudes proportional to N^2. However, in the presence of cavity losses, the final amplitudes greatly depend on these losses, and higher-order resonances reach lower amplitudes due to longer travel in the cavity.

For this experiment, the SUNSHINE facility produces electron pulses at 10 Hz containing a train of about 3000 electron bunches at an energy of 30 MeV. Each bunch has about 2×10^8 electrons within a bunch length of about 200 μm. The inter-bunch distance is 10.5 cm. By detecting radiation wavelengths longer than or equal to the bunch length, we are able to observe stimulated coherent transition radiation in the far-infrared regime with a room-temperature bolometer.

The simplified schematic diagram of the experimental realization of the BRAICER cavity is shown in Fig. 2. It consists of a foil radiator/reflector (R), two foil reflectors (F1 and F2), two Au-coated off-axis parabolic reflectors of 152-mm effective focal length (P1 and P2), two Au-coated first-surface mirrors (M1 and M2), and a 127-μm-thick Mylar beam splitter supported by an Al ring (BS). All foil reflectors (R, F1 and F2) are made of 8-μm-thick Al foils supported by Al rings. The focal points of P1 and P2 are aligned with the surfaces of R and with each other. The mirrors (M1 and M2) and the beam splitter (BS) are mounted to a remote-controlled linear translation stage. This allows us to change the loop length without affecting the alignment. Some radiation is coupled out by the beam splitter and collected into a room-temperature pyroelectric bolometer through a copper cone [3]. Presently, the whole cavity is placed in air. The electrons are extracted from the evacuated beam line through a 75-μm-thick stainless steel window. They cross the cavity (via F2, R, and F1), and are finally absorbed into a beam dump. We simplify the assembly and alignment problems by placing the cavity in air, but suffer from multiple scattering problems caused by electrons passing through the stainless steel window and the air, which reduces the radiation signal. Additionally, radiation is absorbed significantly by humidity resulting in large cavity losses. Forward transition radiation emitted from F2 and the backward one emitted from F1 will not be amplified by the cavity because of geometry but will contribute to the background. This is also true for Cherenkov radiation emitted in the air.

By performing detuning measurements on the cavity, we are able to scan through its different resonances. This detuning procedure is carried out by measuring radiated energy into the bolometer as a function of the loop length. A typical detuning scan is shown in Fig. 3(a) where the loop length varies from $7\frac{1}{2}d_{ib}$ to $8d_{ib}$. Three resonances are observed in this range located at $7\frac{1}{2}d_{ib}$, $7\frac{3}{4}d_{ib}$, and $8d_{ib}$. A theoretical prediction for a perfectly aligned cavity-beam system, in which the electron bunches cross the focal points of P1 and P2 (c.f., Fig. 1), is shown in Fig. 3(b). The simulation uses electron beam parameters mentioned above along with the assumptions of uniform particle distribution and 70% cavity losses, which are chosen to match the measurements. Although the second-order resonance at $7\frac{1}{2}d_{ib}$ and the fourth-order resonance at $7\frac{3}{4}d_{ib}$ agree with theory, there are still two major discrepancies between the two results: (1) the third-order resonance at $7\frac{2}{3}d_{ib}$ in the measurement does not show the expected amplitude predicted by theory, and (2) the resonances at $8d_{ib}$ in both results behave differently.

By inspecting the oxidation trace on R, F1, and F2 caused by the electrons, we conclude that the electrons pass through R with an offset from the focal points of P1 and P2. This misaligned case is demonstrated in Fig. 4. Some of the resonances will be affected by this misalignment. For example, if the loop length is an integral (say n) multiple of d_{ib}, the radiation emitted from some bunch at C after a travel around the cavity will not meet the next n^{th} bunch at D because the image point of C is displaced to I; however, this radiation will travel back to C to meet the next $2n^{th}$ bunch with two-loop-length-long travel. This is exactly the *second*-order resonance, instead of the first order. Resonances at half-multiples of d_{ib} will remain of second order. In general, odd-order resonances (say n^{th}) will in this case become even order ($2n^{th}$), while all even-order resonances remain the same. The theoretical simulation of the misalignment effects is shown in Fig. 3(c) and agrees with the measured scan. The absence of odd-order resonances also strongly indicates that the measured resonant peaks are real stimulation of radiation, instead of the interference effects between radiation pulses. For example, at $7\frac{2}{3}d_{ib}(=\frac{23}{3}d_{ib})$ the radiation emitted from C by a bunch after three-loop-length-long travel will co-propagate in the cavity with the radiation emitted from D by the next 23^{rd} bunch. No interference effects due to these two co-moving pulses are observed at this loop length, and the resulting 6^{th} order resonance is too small to have a clear observation.

In this Letter, we have described the principle and the experimental setup of a BRAICER cavity. By performing a detuning scan of the cavity, we demonstrated resonant conditions of the cavity. These resonances along with theoretical simulations confirm the observation of stimulated transition radiation for the first time. This implies that a BRAICER cavity can be used to generate high-power, coherent far-infrared radiation through stimulated emission of transition radiation. To achieve this, a new vacuum-compatible cavity design is required that greatly eliminates losses and the scattering of the electron beam through a stainless steel window. A more detailed publication including the theory of the BRAICER cavity and a proposed fast Q-switched BRAICER cavity is under preparation. This work is supported by Department of Energy contract DE–AC03–76F00515.

---

[1] Y. N. Istomin and A. V. Luk'yanov, Sov. Phys. JETP **70**, 891(1990).
[2] V. L. Ginzburg and V. N. Tsytovich, *Transition Radiation and Transition Scattering* (Adam Hilger, Bristol, 1990).
[3] P. Kung, H. C. Lihn, D. Bocek, and H. Wiedemann, Proc. SPIE **2118**, 191(1994).
[4] P. Kung, H. C. Lihn, D. Bocek, and H. Wiedemann, Phys. Rev. Lett. **73**, 967(1994).
[5] J. S. Nodvic and D. S. Saxon, Phys. Rev. **96**, 180(1954).

FIG. 1. Conceptual schematic diagram of the BRAICER cavity.

FIG. 2. Simplified schematic diagram of the experimental realization of the BRAICER cavity.

FIG. 3. Typical experimental and theoretical detuning scans of the BRAICER cavity. An experimental scan is shown in (a) where the loop length varies from $7\frac{1}{2}d_{ib}$ to $8d_{ib}$. Note that a change of δ in the beam-splitter position corresponds to 2δ in actual loop length. Theoretical predictions are shown in (b) for a perfectly aligned case and in (c) for a misaligned case.

FIG. 4. A misaligned BRAICER cavity in which the electron bunches cross R (at C and D) with an offset from the optical axis defined by the focal points of P1 and P2. The image points of C and D are displaced to I and J, respectively.

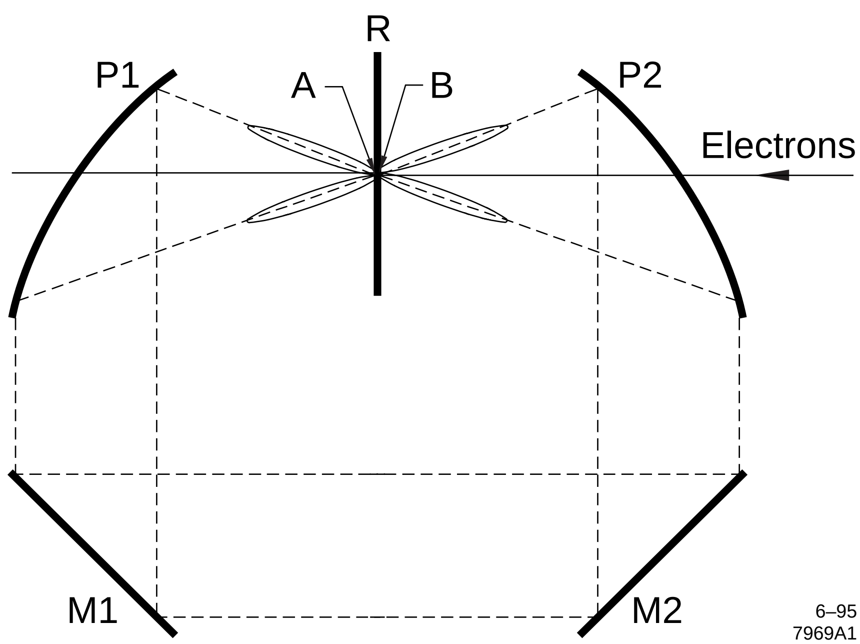

Figure 1

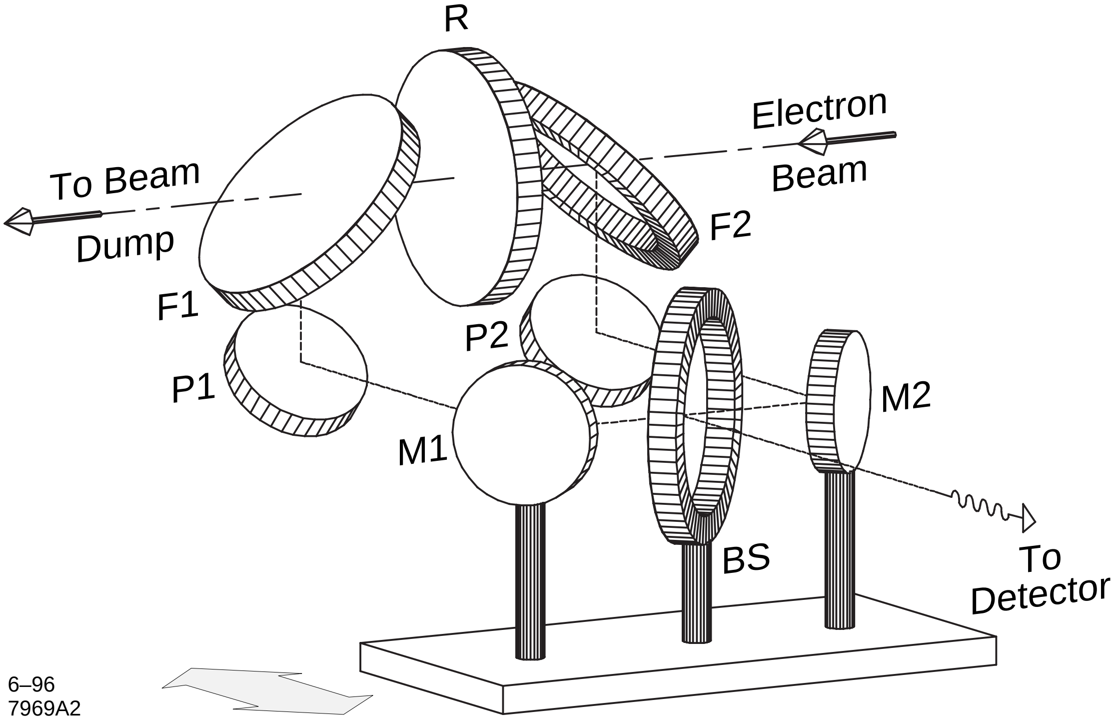
R
Electron
Beam
To Beam
Dump
F2
F1
P2
P1
M2
M1
BS
To
Detector
6–96
7969A2

Figure 2

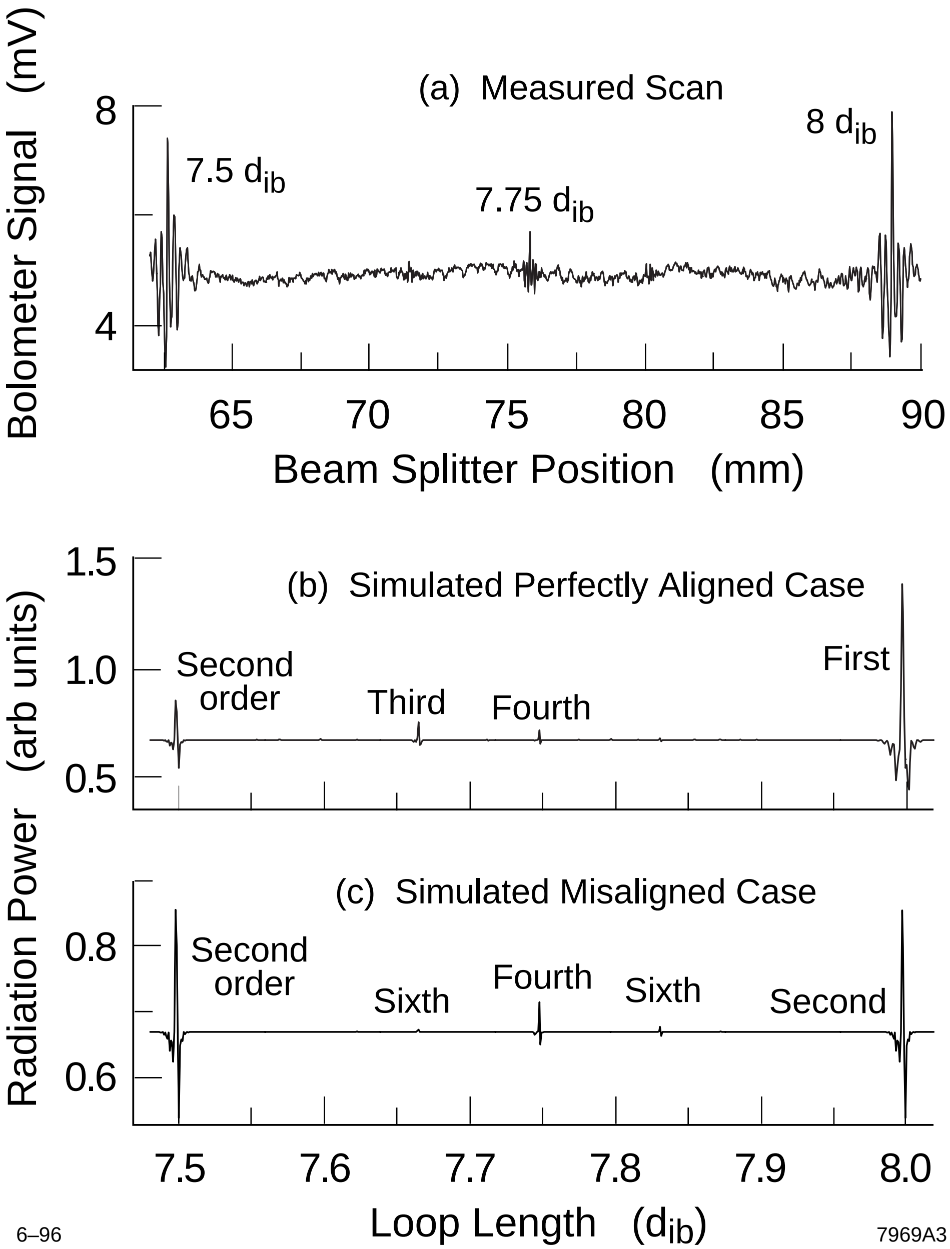

(a) Measured Scan
Bolometer Signal (mV)
8
4
7.5 d_ib
7.75 d_ib
8 d_ib
65
70
75
80
85
90
Beam Splitter Position (mm)
(b) Simulated Perfectly Aligned Case
1.5
1.0
0.5
Second order
Third
Fourth
First
Radiation Power (arb units)
(c) Simulated Misaligned Case
0.8
0.6
Second order
Sixth
Fourth
Sixth
Second
7.5
7.6
7.7
7.8
7.9
8.0
Loop Length (d_ib)
6–96
7969A3

Figure 3

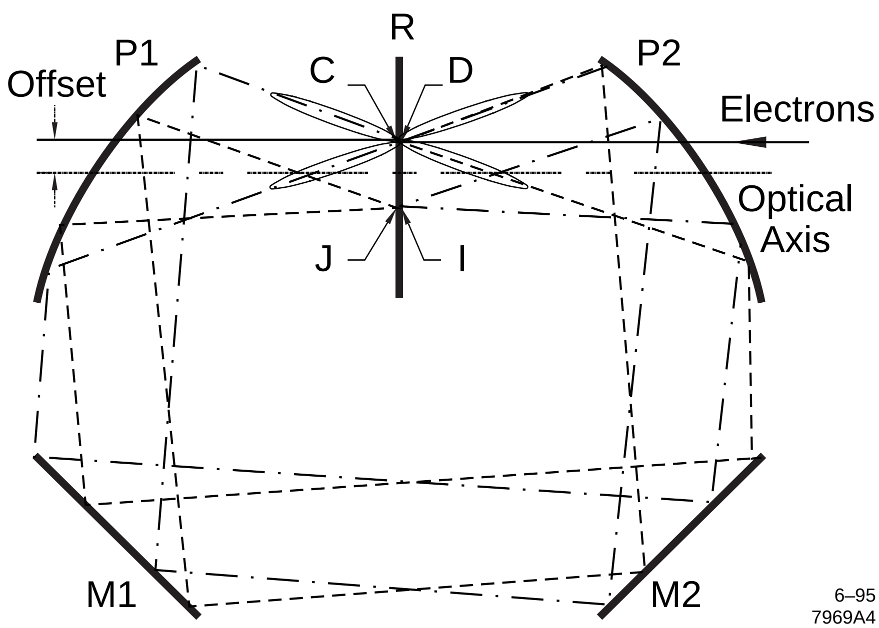

Figure 4